# Particle Formation in Precipitation Polymerization: Continuous Precipitation Polymerization of Acrylic Acid in Supercritical Carbon Dioxide

**Tao Liu,[†] Pamela Garner,[‡] Joseph M. DeSimone,[†,§] George W. Roberts,*[,†] and Geoffrey D. Bothun[‡]**

*Department of Chemical and Biomolecular Engineering, Campus Box 7905, North Carolina State University, Raleigh, North Carolina 27695; Department of Mechanical and Chemical Engineering, 618 McNair Hall, North Carolina A&T State University, Greensboro, North Carolina 27411; and Department of Chemistry, CB #3290, University of North Carolina at Chapel Hill, Chapel Hill, North Carolina 27599-3290*

*Received June 6, 2006; Revised Manuscript Received July 21, 2006*

ABSTRACT: The morphology of the polymer produced during continuous precipitation polymerization of acrylic acid in supercritical carbon dioxide ($scCO_2$) varied significantly with reaction conditions. Three different morphologies were observed: a coagulum of primary particles with diameters of 100−200 nm, irregular particles with diameters of 5−20 $\mu$m, and spheres with diameters of 10−100 $\mu$m. To explore the variables that control particle morphology, the glass transition temperature ($T_g$) of poly(acrylic acid) (PAA) was measured at several $CO_2$ pressures using high-pressure differential scanning calorimetry. Sorption of $scCO_2$ into PAA also was measured at various temperatures and pressures with a quartz crystal microbalance. Chow's equation described the $T_g$ reduction by $CO_2$ quite accurately. Formation of large spherical particles of PAA was favored when the polymer molecular weight was relatively low and when the polymerization temperature was well above $T_g$.

## Introduction

Acrylic acid polymers are widely used as dispersants, thickeners, flocculants, and superabsorbent polymers.[1] Poly(acrylic acid) (PAA) commonly is prepared by aqueous solution polymerization, although heterogeneous polymerizations in organic media also are used.[1]

Interest in understanding the behavior of precipitation polymerizations has been stimulated by use of supercritical carbon dioxide ($scCO_2$) as a polymerization medium.[2,3] Precipitation polymerization of acrylic acid in supercritical carbon dioxide ($scCO_2$) was first reported in a French patent in 1968;[4] a U.S. version of this patent issued in 1970.[5] A Canadian patent application in 1986 described the synthesis of water-soluble PAA in $scCO_2$.[6] In 1988, the synthesis in $scCO_2$ of thickeners based on cross-linked, water-soluble PAA was reported in a U.S. patent,[7] and a similar study was reported in a 1989 European patent.[8] More recently, Romack et al.[9] and Xu and co-workers[10,11] explored other aspects of the polymerization of acrylic acid in $scCO_2$, including the effect of cosolvents.

Most of the previous studies of acrylic acid polymerization were carried out in batch reactors. The products were white, fluffy, fine powders. The polymer particles were a coagulum of primary particles about 100−200 nm in diameter.[9−11] Particles this small can create dusting problems in manufacturing. Dust may be a source of industrial hygiene risks for workers and may pose difficult materials-handling problems. Recently, continuous precipitation polymerization of acrylic acid in $scCO_2$ was carried out in a continuous stirred tank reactor (CSTR).[12−14] For the first time, PAA spheres with diameters of 10−100 $\mu$m were prepared under certain conditions. This paper describes the relationship between polymer morphology and the polymerization conditions. A particle formation mechanism is proposed that is consistent with the experimental data. The central feature of this mechanism is the relationship between polymerization temperature and the glass transition temperature of the polymer at reaction conditions.

## Experimental Section

**Materials.** Carbon dioxide (SFC grade, 99.998%) was purchased from National Specialty Gases. The initiator, 2,2′-azobis(2,4-dimethylvaleronitrile) (V-65B; high purity, 98.8%), was donated by Wako Chemicals USA. Acrylic acid (99.5%), toluene (HPLC grade, 99.5%), 1,1,2-trichloro-1,2,2-trifluoroethane (Freon 113; HPLC grade, 99.8%), 4-methoxyphenol (MEHQ, 99%), and methanol (HPLC grade, 99.9%) were purchased from the Fisher Scientific Co. All chemicals were used as received.

**Continuous Polymerization.** The continuous precipitation polymerization of acrylic acid in $scCO_2$ was carried out in a CSTR using V-65B as the free-radical initiator. The reaction temperature was between 50 and 90 °C, the pressure was 207 bar, the average residence time was between 12 and 40 min, and the inlet monomer and initiator concentrations were varied to change the molecular weight of the polymer produced. The reactor was an 800 mL, high-pressure autoclave with a magnetically driven agitator. A heating/cooling fluid was circulated through a jacket on the reactor to control the reaction temperature. A heated control valve functioned as a backpressure regulator to keep the system pressure at the set point. In a typical experiment, three streams ($CO_2$, acrylic acid, and V-65B/Freon 113 solution) were fed continuously into the reactor with individual syringe pumps. The polymerization took place continuously at steady state. Because PAA is essentially insoluble in $scCO_2$,[15] polymer precipitated as it was formed, so that the mixture in the reactor consisted of a continuous, fluid phase and a dispersed, polymer phase. The product stream was withdrawn

[†] North Carolina State University.
[‡] North Carolina A&T State University.
[§] University of North Carolina at Chapel Hill.
* To whom correspondence should be addressed: e-mail groberts@eos.ncsu.edu; Ph +1 919 515-7328; Fax +1 919 513-3465.

10.1021/ma061260p CCC: $33.50 
Published on Web 08/23/2006

**Table 1. Typical Continuous Polymerization Experiments**[a]

| experiment | $T_P$ (°C) | $[M]_{in}$ (mol/L) | $[I]_{in}$ (mol/L) | yield (%) | $M_v$ (kg/mol) | polymer morphology | $T_g$[b] (° C) |
|---|---|---|---|---|---|---|---|
| 1 | 50 | 1.25 | 0.004 | 30.8 | 175 | coagulum | 121 |
| 2 | 70 | 1.25 | 0.001 | 54.5 | 157 | irregular particles | 116 |
| 3 | 70 | 0.50 | 0.006 | 80.8 | 28.9 | spheres | 113 |
| 4 | 90 | 0.25 | 0.006 | 46.1 | 6.9 | spheres | 100 |

[a] Note: $\tau = 25$ min, $P = 207$ bar, agitation speed = 1800 rpm. [b] In atmospheric nitrogen.

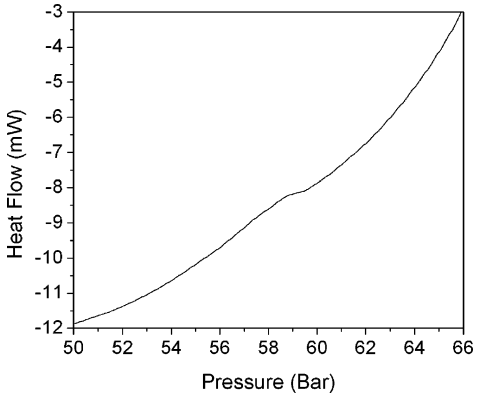


**Figure 1.** An exemplar high-pressure DSC scan at 100 °C.

from the bottom of the reactor and passed through a heat exchanger to cool it to about room temperature. A solution of MEHQ in toluene then was added to stop the polymerization. The polymer particles were collected by filtration and were extracted with liquid $CO_2$ to remove unreacted monomer, initiator, Freon 113, toluene, and MEHQ. Detailed descriptions of the apparatus and polymerization procedure are available elsewhere.[12,16]

The viscosity-average molecular weight ($M_v$) of the polymer was measured with an automatic viscometer (Rheotek TCB-7).[12] The polymer morphologies were determined with scanning electron micrography (SEM, JEOL 6400F Field Emission).

**Differential Scanning Calorimeter (DSC) Measurements. Atmospheric Nitrogen.** The glass transition temperature of pure PAA was measured in atmospheric nitrogen with a TA Instruments Q-100 DSC. Polymer samples (4−8 mg), which had been dried in a vacuum oven for 2 days at 80 °C, were analyzed in crimped aluminum pans under a purge of dry nitrogen at atmospheric pressure and a flow rate of 50 mL/min. The sample history was erased by heating the sample to 180 °C at a heating rate of 10 °C/min and cooling it rapidly (20 °C/min) to −40 °C. A DSC scan then was carried out in the temperature range from −40 to 180 °C at a heating rate of 10 °C/min to determine the glass transition temperature of the pure polymer, $T_{g0}$. The $T_{g0}$ determined for two samples of the same polymer were within ±0.1 °C.

**Supercritical Carbon Dioxide.** The $T_g$ of PAA ($M_v = 175$ kg/mol; experiment 1 in Table 1) in $scCO_2$ was measured with a C80 II Setaram calorimeter operating in an isothermal mode. In this procedure, the $CO_2$ pressure at which the glass transition occurred was determined at a specified temperature. Approximately 70 mg of PAA was placed in a custom-designed, high-pressure sample cell. Carbon dioxide was introduced to the cell using a syringe pump that was preequilibrated at 45 °C in order to prevent a liquid/supercritical phase transition during the DSC scans. The polymer sample was equilibrated for 2 h with $CO_2$ at the desired temperature and pressure (e.g., 80 °C and 173 bar). Then the $CO_2$ pressure was reduced at a rate of 3.4 bar/min to determine the glass transition pressure ($P_g$) at the specified temperature. Three experiments were carried out at each temperature to minimize the error of measurement.

Figure 1 shows a typical DSC scan at 100 °C. In this figure, the plateau of the curve at $P = 59$ bar indicates the occurrence of the glass transition. Therefore, $P_g$ is 59 bar at 100 °C; i.e., $T_g$ is 100 °C at a $CO_2$ pressure of 59 bar.

**Quartz Crystal Microbalance (QCM) Measurements.** This technique is a powerful tool for the study of $CO_2$ absorption into polymers[17−22] due to its accuracy and ease of operation. The apparatus used in this research was comprised of a quartz crystal mounted in a high-pressure cell, a temperature-controlled water bath, an oscillator, and a data-acquisition system. The quartz crystal was a 5 MHz AT-cut Si with gold electrodes (model #131223, International Crystal Manufacturing). The oscillator (PLO-10, Maxtek Inc.) could be operated in the 3−6 MHz frequency range. The high-pressure cell was rated for pressures up to about 500 bar. The water bath could be controlled in the range from room temperature to 90 °C, with an accuracy of ±0.1 °C.

A PAA solution was prepared by dissolving 0.15 g of polymer ($M_v = 175$ kg/mol, experiment 1 in Table 1) in 15 g of methanol. Prior to coating a polymer film on the crystal, the blank crystal was mounted in the QCM apparatus to determine the fundamental frequency in a vacuum at the experimental temperature. After that, the crystal was dipped vertically into the PAA/methanol solution for several minutes. Then it was withdrawn from the solution. The crystal was suspended horizontally for a few minutes to allow the methanol to evaporate. The coated crystal then was mounted in the pressure cell and dried at the experimental temperature under vacuum until the frequency became constant, indicating complete removal of the solvent. The stabilized frequency was used to calculate the polymer mass deposited on the crystal. Carbon dioxide then was added into the high-pressure cell until the pressure reached the desired value. After 1 h, the frequency was essentially constant. At this point, the pressure was increased by introducing more $CO_2$ into the cell, and another sorption equilibrium was obtained. At the completion of an isotherm, the $CO_2$ was released and vacuum was utilized to degas the film. Additional measurements then were carried out at different temperatures.

In addition to $CO_2$, other components of the polymerization mixture, such as unreacted monomer and initiator, also could have been absorbed by the polymer in the reactor. However, the concentrations of these other components were very low relative to $CO_2$. For example, the highest mole fraction of unreacted acrylic acid monomer in the polymerizations was less than 5% of the $CO_2$ mole fraction. Therefore, the measured values of the glass-transition temperature and equilibrium sorption in pure $CO_2$ should be representative of the behavior of the polymer in the reactor.

## Results and Discussion

Some typical polymerization experiments are listed in Table 1. All product polymers were white, dry powders. Experiment 1 was carried out at 50 °C. The viscosity-average molecular weight of the polymer was 175 kg/mol. Figure 2 shows that the polymer produced in this experiment was a coagulum of primary particles about 100−200 nm in diameter. As noted in the Experimental Section, samples of this polymer were used to measure $T_{g0}$, $T_g$, and the mass of $CO_2$ adsorbed.

Experiment 2 was carried out at 70 °C. The polymer molecular weight was 157 kg/mol. Figure 3 shows that the product consisted of irregular particles, with sizes in the range of 5−20 $\mu$m.

Experiment 3 also was carried out at 70 °C, but with a lower inlet monomer concentration ($[M]_{in}$) and a higher inlet initiator concentration ($[I]_{in}$). Accordingly, a lower molecular weight, 28.9 kg/mol, was produced. Figure 4 shows that the polymer particles were spheres about 10−100 $\mu$m in diameter.

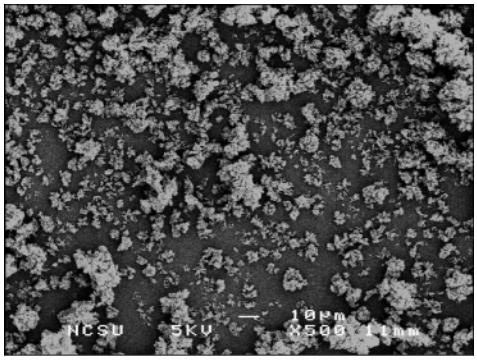


(a)

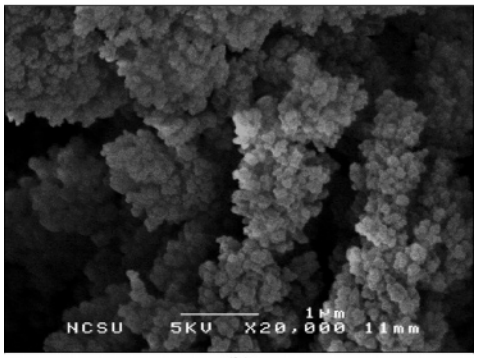


(b)

**Figure 2.** SEM of PAA particles produced in a CSTR polymerization (experiment 1; $T = 50$ °C, $P = 207$ bar, $\tau = 25$ min, $[M]_{in} = 1.25$ mol/L, $[I]_{in} = 0.004$ mol/L, $M_v = 175$ kg/mol): (a) ×500; (b) ×20000.

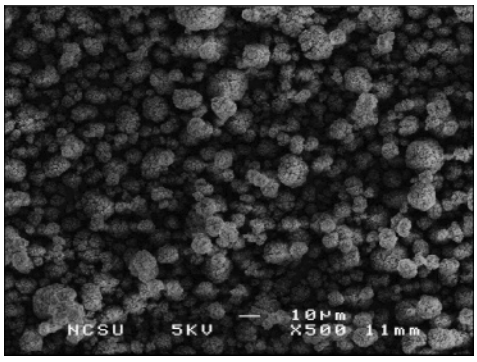


**Figure 3.** SEM of PAA particles produced in a CSTR polymerization (experiment 2; $T = 70$ °C, $P = 207$ bar, $\tau = 25$ min, $[M]_{in} = 1.25$ mol/L, $[I]_{in} = 0.001$ mol/L, $M_v = 157$ kg/mol).

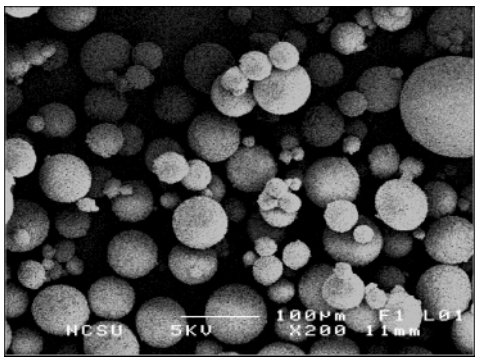


**Figure 4.** SEM of PAA particles produced in a CSTR polymerization (experiment 3; $T = 70$ °C, $P = 207$ bar, $\tau = 25$ min, $[M]_{in} = 0.50$ mol/L, $[I]_{in} = 0.006$ mol/L, $M_v = 28.9$ kg/mol).

Experiment 4 was carried out at 90 °C. The lowest molecular weight (6.9 kg/mol) was obtained, as this experiment was conducted at the highest temperature, the highest initiator concentration, and the lowest monomer concentration. Figure 5 shows that the polymer particles were spheres about 10−100 μm in diameter, similar to those formed in experiment 3.

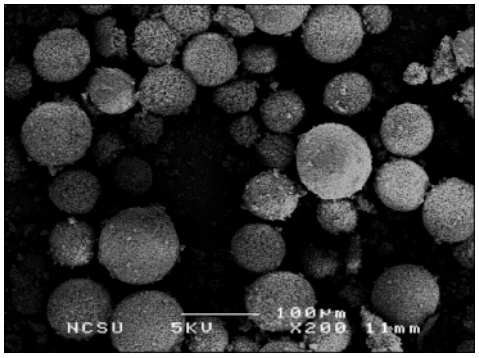


**Figure 5.** SEM of PAA particles produced in a CSTR polymerization (experiment 4; $T = 90$ °C, $P = 207$ bar, $\tau = 25$ min, $[M]_{in} = 0.25$ mol/L, $[I]_{in} = 0.006$ mol/L, $M_v = 6.9$ kg/mol).

The polymer morphologies reported in the literature, such as those by Romack et al.[9] and Xu et al.,[10,11] are coagulum, similar to what is shown in Figure 2. This is the first time that much larger PAA particles have been prepared by precipitation polymerization of acrylic acid in $scCO_2$.

The glass transition temperatures of these four samples of PAA were measured in atmospheric $N_2$. The results are given in Table 1. These values of $T_g$ decrease with molecular weight but are higher than the polymerization temperature in all four cases.

It appears that the polymerization temperature and/or the polymer molecular weight are major factors that affect the polymer morphology. The polymerization temperature in this work was between 50 and 90 °C, which is much lower than the glass transition temperature of pure PAA (i.e, $T_g$ in atmospheric $N_2$), which is reported to be between 106 and 126 °C.[23] However, the presence of sorbed $scCO_2$ in the polymer can decrease its glass transition temperature significantly.[24−31] In the present work, polymer particles formed and precipitated from a high-pressure $CO_2$ phase. The polymer contained dissolved $CO_2$ at a concentration that was essentially in equilibrium with the $CO_2$ in the supercritical fluid.

Chow[32] has proposed a means to calculate the depression of $T_g$ due to a dissolved component:

$$\ln\left(\frac{T_g}{T_{g0}}\right) = \beta[\theta \ln \theta + (1 - \theta)\ln(1 - \theta)]$$

where

$$\theta = \frac{M_p}{zM_d}\frac{\omega}{1 - \omega}$$

$$\beta = \frac{zR}{M_p \Delta C_p}$$

In the above equations, $T_{g0}$ is the glass transition temperature of pure polymer, $T_g$ is the glass transition temperature of the polymer containing solute, $M_p$ is the molar mass of the polymer repeat unit, $M_d$ is the molar mass of the solute, $R$ is the gas constant, $\omega$ is the concentration of solute in the polymer (mass solute/mass polymer), $\Delta C_p$ is the heat capacity change associated with the glass transition of the pure polymer, and $z$ is the lattice coordination number. This parameter can be either 1 or 2. For polymers with small repeat units, such as polystyrene and poly(methyl methacrylate), $z = 1$ gives a good fit of the experimental

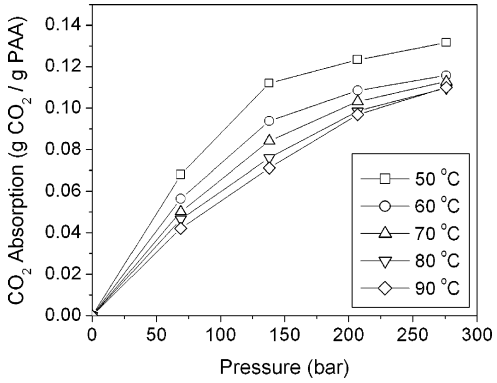


**Figure 6.** $CO_2$ absorption into PAA measured with a QCM.

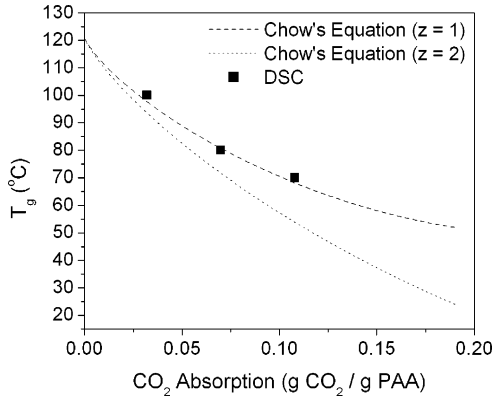


**Figure 7.** $T_g$ of PAA calculated with Chow's equation ($T_{g0}$ = 120.9 °C, $\Delta C_p$ = 0.4 J/(g °C)) compared with measured values from Table 2.

**Table 2. Glass Transition Temperature ($T_g$) of PAA Measured with a High-Pressure DSC in the Presence of $CO_2$**

| $P$ (bar) | $T_g$ (°C) | $\omega$ (g of $CO_2$/g of PAA) |
|---|---|---|
| 59 ± 1 | 100 | 0.032 |
| 124 ± 5 | 80 | 0.070 |
| 211 ± 2 | 70 | 0.11 |

results. For polymers with larger repeat units, such as polycarbonate and poly(ethylene terephthalate), $z$ = 2 usually gives a better description of the data.[24−28] For the PAA prepared in experiment 1 in Table 1, DSC measurements showed that $T_{g0}$ = 120.9 °C and $\Delta C_p$ = 0.4 J/(g °C).

The equilibrium solubilities of $CO_2$ in PAA, as measured with the QCM at various temperatures, are shown in Figure 6. The data in this figure cover the ranges of temperature and pressure that were used in the experiments shown in Table 1. The $CO_2$ solubility decreases with increasing temperature and increases with increasing $CO_2$ pressure.

As shown in Table 2, the glass transition temperatures of PAA in the presence of $CO_2$ decrease with increasing $CO_2$ pressure. The equilibrium $CO_2$ concentrations ($\omega$) that correspond to the glass-transition conditions were determined by interpolation from Figure 6 and are shown in the third column of Table 2. The three data points in Table 2 are compared with the $T_g$ calculated with Chow's equation in Figure 7. Chow's equation agrees with the experimental data very well when $z$ = 1.

Kikic et al.[30] have reported a $T_g$ for PAA of 48 °C at a $CO_2$ pressure of 80 bar. This is substantially below all of the values in Table 2, including the value of 70 °C at the highest $CO_2$ pressure of 211 bar. The PAA used in their study was reported by the supplier to have a $T_{g0}$ of 106 °C, lower than the value of 121 °C for the polymer used for the measurements in Table 2.

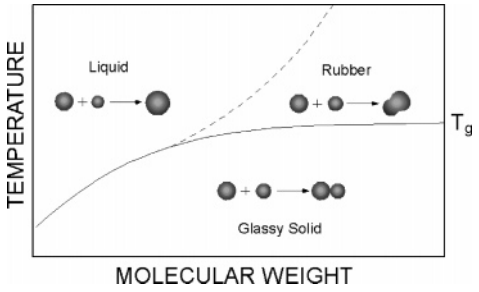


**Figure 8.** A hypothetical particle formation mechanism (adapted from refs 33 and 34).

**Table 3. Comparison of the Polymerization Temperature ($T_P$) with the Polymer Glass Transition Temperature ($T_g$) Estimated with Chow's Equation ($z$ = 1, $T_{g0}$ = 120.9 °C, $\Delta C_p$ = 0.4 J/(g °C))**

| $T_P$ (°C) | $P$ (bar) | $\omega$ (g of $CO_2$/g of PAA) | $T_g$ (°C) |
|---|---|---|---|
| 50 | 207 | 0.12 | 65 |
| 70 | 207 | 0.11 | 68 |
| 90 | 207 | 0.097 | 71 |

Moreover, Kikic et al. used a different technique, inverse gas chromatography, to measure $T_g$. This technique consistently gave somewhat lower $T_g$'s in atmospheric $N_2$ than DSC. For example, Kikic et al. measured a $T_g$ of 100 °C for their PAA compared to the supplier value of 106 °C.

In an attempt to rationalize the apparent discrepancy between the previous and present results, the sorption of $CO_2$ into PAA at 80 bar and 48 °C was estimated from Figure 6. Chow's equation then was used to estimate $T_g$ for PAA with a $T_{g0}$ of 100 °C and a $\Delta C_p$ of 0.4 J/(g °C) at 80 bar of $CO_2$ pressure. The result was $T_g$ = 59 °C, about 11 °C higher than the value of Kikic et al.,[30] but much closer to it than suggested by a cursory examination of Table 2. The remaining difference may be the result of differences between the two polymers, such that Figure 6 may not provide an accurate estimate of $\omega$ for the PAA of Kikic et al. or that $\Delta C_p \neq$ 0.4 J/(g °C) for their polymer.

The $T_g$ of PAA, at the polymerization conditions given in Table 1, was estimated from Chow's equation, using values of $\omega$ obtained from Figure 6. Table 3 compares the polymerization temperature, $T_P$, with the estimated $T_g$ at the conditions of the each experiment. The estimated values of $T_g$ should apply closely to the polymers produced in experiments 1 and 2 of Table 1 because the molecular weights of these two polymers were the same as, or close to, the molecular weight of the polymer used in the DSC and QCM experiments that validated Chow's equation. However, the $T_g$'s in Table 3 may be higher than the actual $T_g$s of the polymers produced in experiments 3 and 4. The molecular weights of the polymers produced in these two experiments were substantially lower than the molecular weight of the polymer used in the DSC and QCM experiments.

At 50 °C and 207 bar (experiment 1), $T_P$ is about 15 °C lower than the estimated value of $T_g$. At 90 °C and 207 bar (experiment 4), $T_P$ is at least 19 °C higher than $T_g$. Finally, at 70 °C and 207 bar, $T_P$ is just 2 °C higher than $T_g$, for the higher $M_v$ polymer (experiment 2) and perhaps somewhat higher than 2 °C for the lower $M_v$ polymer (experiment 3).

Figure 8 shows a hypothetical particle formation mechanism. For an amorphous polymer, $T_g$ increases with molecular weight when the molecular weight is low and levels off at higher molecular weights. The polymers synthesized in this work demonstrate this behavior, as shown in Table 1. Depending on temperature and molecular weight, the polymer can be formed in three different physical states: glassy solid, liquid, or rubber.[33] In these experiments, when the polymerization temperature, $T_P$, was below $T_g$, the precipitated polymer was in the glassy state.

The glassy particles probably had little or no tendency to coalesce when they collided and remained as small, irregular primary particles. This is consistent with the observed morphology of the polymer produced in experiment 1 in Table 1. When $T_P$ was above $T_g$, and the polymer molecular weight was low, the polymer probably was present in the reactor as droplets of a viscous liquid. These droplets should have been able to coalesce to form larger, spherical particles. In this case, the intensity of agitation would be expected to affect the particle size distribution. After the product stream was withdrawn from the reactor, it was cooled to approximately room temperature, much lower than $T_g$, so that the polymer solidified. This describes the conditions of experiment 4 in Table 1 and perhaps those of experiment 3.

When $T_P$ was above $T_g$ and the polymer molecular weight was high, as in experiment 2, the polymer was formed in a rubbery state. The primary particles might have had some tendency to stick to each other when they collided, but their coalescence probably was more difficult. It is believed that the irregular particles were formed in this case. Again, the intensity of agitation should have an effect at this condition. An example of the influence of agitation on particle morphology is provided by the work of Tai et al.,[34] which is discussed below.

The hypothesis outlined above suggests that the morphology of the polymer particles produced during precipitation polymerization in $scCO_2$ can be controlled by adjusting the polymerization temperature and/or the $CO_2$ pressure. In particular, the hypothesis suggests that higher $CO_2$ pressures should lead to lower values of $T_g$ and to larger, more spherical polymer particles. Larger particles also appear to be favored by lower molecular weights. However, reducing the molecular weight may not be a practical alternative in view of the influence of this parameter on other polymer properties.

To test the generality of the hypothesis represented in Figure 8, three previously published studies of particle morphology have been analyzed. One study involved PAA, and the other two concerned poly(vinylidene fluoride) (PVDF). The polymerization of vinylidene fluoride monomer to form PVDF is one of the most studied precipitation polymerizations in $scCO_2$.

As noted previously, Romack et al.[9] carried out the precipitation polymerization of acrylic acid in $scCO_2$, at a temperature of 62 °C and at $CO_2$ pressures between 125 and 345 bar. Scanning electron micrographs of the polymers produced at these two pressures show that the product was a coagulum consisting of primary particles with diameters on the order of 100 nm, similar to the polymer shown in Figure 2. The glass transition temperature of PAA at 125 bar was estimated to be about 75 °C, using Figure 6 and Chow's equation. Thus, the polymerization temperature, 62 °C, was substantially lower than the estimated $T_g$ of the polymer at reaction conditions. Clearly, the morphology of the product produced at 125 bar was consistent with the present hypothesis. A value of $T_g$ at 345 bar was not estimated because a significant extrapolation of the data in Figure 6 would have been required.

The morphology of PVDF produced by precipitation polymerization in $scCO_2$ has been reported by Charpentier et al.[35] and by Tai et al.[34] In fact, particle morphology was the primary focus of the latter study. The glass transition temperature of PVDF, in the absence of any sorbed species, is about −35 °C. Precipitation polymerizations in $scCO_2$ have been conducted at temperatures from about 40 to about 90 °C, substantially higher than $T_g$ at polymerization conditions. Therefore, the present hypothesis suggests that small PVDF particles would tend to coalesce into larger ones. However, PVDF has a crystallinity of about 60%, and the melting point of the crystallites is in the range of 155−192 °C. Therefore, only about 40% of the PVDF is molten or rubbery at typical polymerization temperatures.

Charpentier et al.[35] show SEMs of the PVDF particles produced in one of their experiments in a continuous stirred-tank reactor. The particles appear to have a wide range of sizes, with a typical value of about 20 $\mu$m. They are irregular in shape and have a very rough surface. The size and appearance of these particles are consistent with the hypothesis of agglomeration of smaller primary particles.

Tai et al.[34] carried out an extensive investigation of the factors that influence the morphology of PVDF particles formed by precipitation polymerization in $scCO_2$, using a stirred batch reactor. The size of the formed particles depended strongly on the concentration of vinylidene fluoride monomer, on the stirring rate, and on the agitator design. At monomer concentrations comparable to those used by Charpentier et al.,[35] the sizes of the particles formed in the two investigations were similar. However, as the monomer concentration was increased, the particles became larger and macroporosity developed. At high monomer concentrations, the SEM images showed aggregates of smaller particles.

Not surprisingly, the intensity of agitation also influenced particle morphology in the Tai et al. study. At low stirrer speeds, distinct, nearly spherical particles with a relatively smooth surface were observed when the monomer concentration was high. As the stirrer speed was increased, the particles became smaller, their surface became less regular, and they developed a fibrous appearance.

On balance, the results of these previous studies support the hypothesis of Figure 8, which is, in fact, an extension of one proposed by Tai et al.[34] In particular, it does not appear as though the high crystallinity of PVDF prevents the agglomeration of primary particles under conditions where the polymerization temperature is well above $T_g$ of the amorphous region.

## Conclusions

Continuous precipitation polymerization of acrylic acid in $scCO_2$ was carried out in a CSTR. Three types of polymer morphology were observed, depending on polymerization conditions: a coagulum of primary particles with diameters of 100−200 nm, irregular particles 5−20 $\mu$m in diameter, and spherical particles 10−100 $\mu$m in diameter. The smallest particles were produced when the polymerization temperature, $T_P$, was well below the polymer glass transition temperature, $T_g$, i.e., when the polymer was formed in the glassy state. Larger, but still irregular, particles were formed when $T_P$ was above, but close to, $T_g$, i.e., when the polymer was formed in a rubbery state. The largest spherical particles were produced when $T_P$ was well above $T_g$ and the polymer molecular weight was low, i.e., when the polymer probably was formed in a viscous liquid state. These results appear to be consistent with previous studies of the polymerization of both acrylic acid and vinylidene fluoride in $scCO_2$. The present study suggests that a particular polymer morphology can be obtained through manipulation of the polymerization conditions.

**Acknowledgment.** This research was supported by the Kenan Center for the Utilization of $CO_2$ in Manufacturing at North Carolina State University, the STC Program of the National Science Foundation under Agreement CHE-9876674, and the National Science Foundation Discovery Corps Fellowship Program under Agreement CHE-0412109.

CDV

## Nomenclature

| | |
|---|---|
| $\Delta C_p$ | polymer heat capacity change associated with glass transition (J/(g °C)) |
| $[I]_{in}$ | inlet initiator concentration (mol/L) |
| $M_d$ | molar mass of solute (g/mol) |
| $[M]_{in}$ | inlet monomer concentration (mol/L) |
| $M_p$ | molar mass of polymer repeat unit (g/mol) |
| $M_v$ | viscosity-average molecular weight of polymer (kg/mol) |
| $P$ | pressure (bar) |
| $T_P$ | polymerization temperature (°C) |
| $T_g$ | glass transition temperature of polymer (°C) |
| $T_{g0}$ | glass transition temperature of pure polymer (°C) |
| $z$ | lattice coordination number |
| $\tau$ | average residence time (min) |
| $\omega$ | $CO_2$ absorption into polymer (g of $CO_2$/g of polymer) |

## References and Notes


(1) Swift, G. In *Encyclopedia of Polymer Science and Technology*, 3rd ed.; Bailey, J., Kroschwitz, J. I., Eds. John Wiley & Sons: Hoboken, NJ, 2003; Vol. 10, p 79.
(2) Canelas, D. A.; DeSimone, J. M. *Adv. Polym. Sci.* **1997**, *133*, 103−140.
(3) McCoy, M. *Chem. Eng. News* **1999**, *77*, 10.
(4) Fukui, K.; Fujii, K.; Kagiya, T.; Toriuchi, Y.; Yokota, H. French Patent No. 1,524,533, 1968.
(5) Fukui, K.; Fujii, K.; Kagiya, T.; Toriuchi, Y.; Yokota, H. US Patent No. 3,522,228, 1970.
(6) Sertage, W. G. J.; Davis, P.; Schenck, H. U.; Denzinger, W.; Hartmann, H. Canadian Patent No. 1,274,942, 1990.
(7) Hartmann, H.; Denzinger, W. US Patent No. 4,748,220, 1988.
(8) Herbert, M. W.; Huvard, G. S. European Patent No. 0,301,532 (A2), 1989.
(9) Romack, T. J.; Maury, E. E.; Desimone, J. M. *Macromolecules* **1995**, *28*, , 912−915.
(10) Xu, Q.; Han, B.; Yan, H. *Polymer* **2001**, *42*, 1369−1373.
(11) Xu, Q.; Han, B.; Yan, H. *J. Appl. Polym. Sci.* **2003**, *88*, 1876−1880.
(12) Liu, T.; DeSimone, J. M.; Roberts, G. W. *J. Polym. Sci., Part A: Polym. Chem.* **2005**, *43*, 2546−2555.
(13) Liu, T.; DeSimone, J. M.; Roberts, G. W. *Chem. Eng. Sci.* **2006**, *61*, 3129−3139.
(14) Liu, T.; DeSimone, J. M.; Roberts, G. W. *Polymer* **2006**, *47*, 4276−4281.
(15) Rindfleisch, F.; DiNoia, T. P.; McHugh, M. A. *J. Phys. Chem.* **1996**, *100*, 15581−15587.
(16) Liu, T. Ph.D. Thesis, North Carolina State University, Raleigh, North Carolina, 2005.
(17) Miura, K.; Otake, K.; Kurosawa, S.; Sako, T.; Sugeta, T.; Nakane, T.; Sato, M.; Tsuji, T.; Hiaki, T.; Hongo, M. *Fluid Phase Equilib.* **1998**, *144*, 181−189.
(18) Zhang, C.; Cappleman, B. P.; Defibaugh-Chavez, M.; Weinkauf, D. H. *J. Polym. Sci., Part B: Polym. Phys.* **2003**, *41*, 2109−2118.
(19) Aubert, J. H. *J. Supercrit. Fluids* **1998**, *11*, 163−172.
(20) Park, K. H.; Koh, M. S.; Yoon, C. H.; Kim, H. W.; Kim, H. D. *J. Supercrit. Fluids* **2004**, *29*, 203-212.
(21) Wu, Y. T.; Akoto-Ampaw, P. J.; Elbaccouch, M.; Hurrey, M. L.; Wallen, S. L.; Grant, C. S. *Langmuir* **2004**, *20*, 3665−3673.
(22) Wu, Y. T.; Grant, C. S. In *Dekker Encyclopedia of Nanoscience and Nanotechnolgy*; Schwarz, J. A., Contescu, C. I., Putyera, K., Eds.; Marcel Dekker: New York, 2004; p 1977.
(23) Buchholz, F. L.; Graham, A. T. In *Industrial Polymers Handbook—Products, Processes, Applications*; Wilks, E. S., Ed.; Wiley-VCH: Weinheim, 2000; Vol. 1, p 565.
(24) Chiou, J. S.; Barlow, J. W.; Paul, D. R. *J. Appl. Polym. Sci.* **1985**, *30*, 2633−2642.
(25) Handa, Y. P.; Capowski, S.; Oneill, M. *Thermochim. Acta* **1993**, *226*, 177−185.
(26) Banerjee, T.; Lipscomb, G. C. *J. Appl. Polym. Sci.* **1998**, *68*, 1441−1449.
(27) Handa, Y. P.; Lampron, S.; O'Neill, M. L. *J. Polym. Sci., Part B: Polym. Phys.* **1994**, *32*, 2549−2553.
(28) Chiou, J. S.; Paul, D. R. *J. Appl. Polym. Sci.* **1986**, *32*, 2897−2981.
(29) Bos, A.; Punt, I. G. M.; Wessling, M.; Strathmann, H. *J. Membr. Sci.* **1999**, *155*, 67−78.
(30) Kikic, I.; Vecchione, F.; Alessi, P.; Cortesi, A.; Eva, F. *Ind. Eng. Chem. Res.* **2003**, *42*, 3022−3029.
(31) Alessi, P.; Cortesi, A.; Kikic, I.; Vecchione, F. *J. Appl. Polym. Sci.* **2003**, *88*, 2189−2193.
(32) Chow, T. S. *Macromolecules* **1980**, *13*, 362−364.
(33) Rudin, A. In *The Elements of Polymer Science and Engineering*, 2nd ed.; Academic Press: San Diego, 1998; p 381.
(34) Tai, H.; Liu, J.; Howdle, S. M. *Eur. Polym. J.* **2005**, *41*, 2544−2551.
(35) Charpentier, P. A.; DeSimone, J. M.; Roberts, G. W. *Ind. Eng. Chem. Res.* **2000**, *39*, 4588−4596.


MA061260P